Defence Science Journal, Vol. 56, No. 2, April 2006, pp. 147-158

Computation of Flow through an Annular Diffuser and Volute Exhaust

M. Arun, E.G. Tulapurkara, and T. Sundararajan
Indian Institute of Technology Madras, Chennai–600 036

ABSTRACT

Turbulent flow in a diffuser with swirl occurs in many commonly used fluid mechanical devices,eg, diffusers located downstream of a gas turbine, and in certain types of combustion chambers. Diffusers are widely used for converting kinetic energy to pressure, and a reliable prediction method of such flows with the required flow conditions would lead to the design of fluid machinery with improved efficiency. As a first step, turbulent swirling flow through a 12^{o} included angle conical diffuser for a swirl parameter, $m = 0.18$ was numerically investigated using various turbulence models like standard k-ε, RNG-based k-ε, shear-stress transport (SST) k-ω, and Reynolds stress model (RSM). Though the comparison between the experimental and the predicted mean velocity profile by RSM is superior to that by RNG k-ε and SST models, the latter two models give closer comparison with the experimental pressure distribution. Subsequently, computation of flow inside a complex duct involving axisymmetric annular diffuser, transition from rectangular to circular cross section, and exit pipe have been carried out using RNG k-ε and SST k-ω models. The comparison of computed and experimental results indicates that the SST k-ω model gives predictions with reasonable accuracy.

Keywords: Conical diffuser, annular diffuser, swirl parameter, turbulence models, turbulent flow, computer model, computation, diffusers

NOMENCLATURE

k	Turbulent kinetic energy
p	Pressure
Re	Reynolds number
S	$\sqrt{2S_{ij}S_{ij}}$,Magnitude of the rate-of-strain
t	Time
u', v', w'	Components of fluctuating velocity along X, Y, Z directions
u, v, w	Components of instanteneous velocity along X, Y, Z directions
x, y, z	Cartesian coordinates
α, β	Constants in models of turbulence
δ_{ij}	Kronecker delta
ε	Rate of dissipation of turbulent kinetic energy
ν	Kinematic viscosity
ν_t	Eddy kinematic viscosity $= \mu_t / \rho$
ρ	Density
ω	Specific dissipation rate (ε / k)
Ω	Vorticity
Subscripts	
i, j, k or 1, 2, 3	Quantities in X, Y, Z directions

Superscripts

′ Fluctuating quantities wrt time average

– Time-averaged quantities

1. INTRODUCTION

The objective of the present investigation was to compute turbulent flow in a complex duct located downstream of a gas turbine. These devices are widely used for converting kinetic energy to pressure, and a reliable prediction method of such flows with the required flow conditions would lead to the design of fluid machinery with an improved efficiency.

Arun[1], *et al*. computed turbulent swirling flow in a conical diffuser with and without swirl using various models of turbulence. They found that RNG k-ε model with correction for swirl and shear-stress transport k-ω model gave close agreement with experimentally observed pressure distribution. Arun and Tulapurkara[2] computed turbulent flow inside an enclosure with a central partition with RNG k-ε, RSM, and SST k-ω models.Only SST k-ω model was able to predict the shifting of vortices observed behind the partition in the experiments. In the present investigation, the flow inside a complex duct involving axisymmetric annular diffuser, transition from rectangular to circular cross section, and exit pipe as shown in Fig.1, has been carried out using RNG k-ε and SST k-ω models. The dimensions are not given due to proprietory nature of the configuration.

2. GOVERNING EQUATIONS & TURBULENCE CLOSURE MODELLING

The FLUENT 6.0 computational fluid dynamics software has been used as the platform for the present numerical investigation. The 3-D unsteady, compressible N-S equations, in standard tensorial notation given by the expressions

$$\frac{\partial u_i}{\partial x_i}=0 \tag{1}$$

$$\frac{\partial u_i}{\partial t}+\frac{\partial}{\partial x_j}\left(u_i u_j\right)=-\frac{1}{\rho}\frac{\partial p}{\partial x_i}+\frac{\partial}{\partial x_j}\left(\nu\frac{\partial u_i}{\partial x_j}-\overline{u_i' u_j'}\right) \tag{2}$$

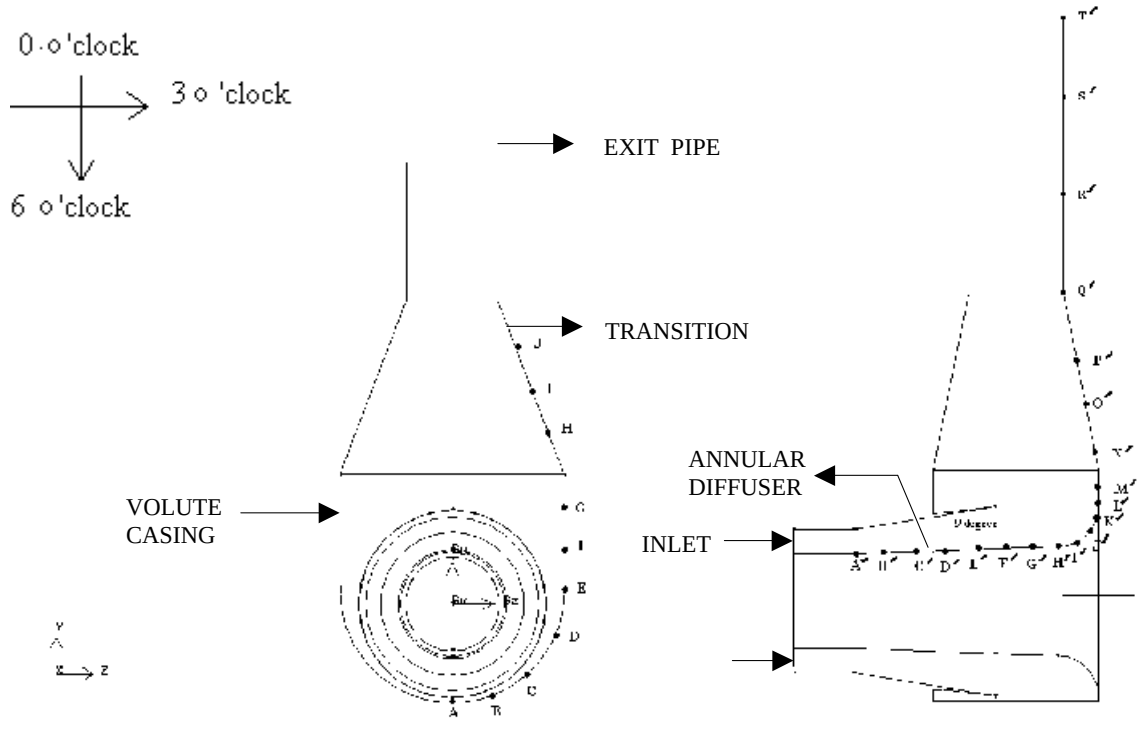

Figure 1. Geometry of complex duct: (a) front view and (b) side view

are solved using finite volume method (FVM). The semi-implicit method for pressure-linked equations (SIMPLE) algorithm is used to solve the coupled pressure and velocity fields with second-order accurate differencing scheme. The models of turbulence are briefly described below.

2.1 RNG-based k-ε Model

The RNG-based k-ε model has a form similar to the standard k-ε model. The transport equations[3] are:

$$\frac{\partial}{\partial t}(k)+\frac{\partial}{\partial x_i}(ku_i)=\frac{\partial}{\partial x_j}\left(\alpha\nu_t\frac{\partial k}{\partial x_j}\right)+\nu_t S^2-\varepsilon \qquad (3)$$

$$\frac{\partial}{\partial t}(\varepsilon)+\frac{\partial}{\partial x_j}(\varepsilon u_j)=\frac{\partial}{\partial x_j}\left(\alpha\nu_t\frac{\partial \varepsilon}{\partial x_j}\right)+C_{1\varepsilon}\frac{\varepsilon}{k}\nu_t S^2-C_{2\varepsilon}\frac{\varepsilon^2}{k}-R_\varepsilon \qquad (4)$$

The quantity α is the inverse effective Prandtl number for k as well as ε. The effective viscosity is calculated using the following:

$$\nu_{eddy}=\nu_{mol}\left[1+\sqrt{\frac{C_\mu}{\nu_{mol}}}\frac{k}{\sqrt{\varepsilon}}\right]^2$$

The turbulent viscosity is given as $\nu_t=(\nu_{eddy}-\nu_{mol})$ and the term R_ε is expressed as

$$R_\varepsilon=\frac{C_\mu\eta^3(1-\eta/\eta_0)}{1+\beta\eta^3}\frac{\varepsilon^2}{k}$$

where $\eta\equiv Sk/\varepsilon,\ \eta_0=4.380,\ \beta=0.012.$

The model constants $C_{1\varepsilon}$, $C_{2\varepsilon}$, and C_μ are 1.42, 1.68, and 0.084, respectively. The inverse effective Prandtl number (α) is computed using the following formula derived analytically in the RNG theory:

$$\left|\frac{\alpha-1.3929}{\alpha_0-1.3929}\right|^{0.6321}\left|\frac{\alpha+2.3929}{\alpha_0+2.3929}\right|^{0.3679}=\frac{\nu_{mol}}{\nu_{eddy}}$$

where α_0 = 1.0. In the high-Reynolds-number limit $\alpha\approx 1.393$.

Thus, the RNG-based model is more responsive to the effects of rapid strain and streamline curvature than the standard k-ε model. A comprehensive description of RNG theory and its application to turbulence can be found in Yakhot and Orszag[3].

2.2 Shear-stress Transport k-ω Model

The shear-stress transport (SST) k-ω model was developed by Menter[4] to effectively blend the robust and accurate formulation of the k-ω model in the near-wall region with the free-stream independence of the k-ε model in the far field.

$$\frac{\partial}{\partial t}(k)+\frac{\partial}{\partial x_i}(ku_i)=\frac{\partial}{\partial x_j}(\Gamma_k\frac{\partial k}{\partial x_j})+\nu_t S^2-Y_k \qquad (5)$$

$$\frac{\partial}{\partial t}(\omega)+\frac{\partial}{\partial x_i}(\omega u_i)=\frac{\partial}{\partial x_j}(\Gamma_\omega\frac{\partial \varepsilon}{\partial x_j})+\alpha S^2-Y_\omega+D_\omega \qquad (6)$$

In these equations, Y_k and Y_ω represent the dissipation of k and ω due to turbulence. D_ω represents the cross-diffusion term. Γ_k and Γ_ω represent the effective diffusivity of k and ω, and are given by

$$\Gamma_k=\nu+\frac{\nu_t}{\sigma_k};\quad \Gamma_\omega=\nu+\frac{\nu_\omega}{\sigma_\omega}$$

where σ_k and σ_ω are the turbulent Prandtl numbers for k and ω:

$$\sigma_\omega=\frac{1}{F_1/\sigma_{\omega,1}+(1-F_1)/\sigma_{\omega,2}}$$

$$\sigma_k=\frac{1}{F_1/\sigma_{k,1}+(1-F_1)/\sigma_{k,2}}$$

respectively. The turbulent viscosity, ν_t is computed as

$$\nu_t=\frac{k}{\omega}\frac{1}{\max\left[\frac{1}{\alpha^*},\frac{\Omega F_2}{\alpha_1\omega}\right]}$$

where $\Omega\equiv\sqrt{2\Omega_{ij}\Omega_{ij}}$ and Ω_{ij} is the mean rate of rotation tensor.

$$\alpha^* = \alpha^*_\infty \left(\frac{\alpha^*_0 + R_{et}/R_k}{1 + R_{et}/R_k} \right)$$

where

$$R_{et} = \frac{\rho k}{\mu \omega}\,;\; R_k = 6.0\,;\quad \alpha^*_0 = \frac{\beta_i}{3.0}\,;\; \beta_i = 0.072\,.$$

The k-ε model is converted into a k-ω formulation using the blending functions, F_1 and F_2 and are given by

$$F_1 = \tanh(\phi_1^4)\,,\; F_2 = \tanh(\phi_2^2)$$

where

$$\phi_1 = \min\left[\max\left(\frac{\sqrt{k}}{0.09\omega y}, \frac{500\mu}{\rho y^2 \omega} \right), \frac{4\rho k}{\sigma_{\omega,2} D^+_\omega y^2} \right]$$

$$\phi_2 = \max\left[2\frac{\sqrt{k}}{0.09\omega y}, \frac{500\mu}{\rho y^2 \omega} \right]$$

$$D^+_\omega = \max\left[2\rho \frac{1}{\sigma_{2,2}} \frac{1}{\omega} \frac{\partial k}{\partial x_j} \frac{\partial \omega}{\partial x_j}, 10^{-20} \right]$$

where y is the distance to the wall surface and D^+_ω is the positive portion of the cross-diffusion term.

The coefficient α in the production term of ω is given by $\alpha = \frac{\alpha_\infty}{\alpha^*}\left(\frac{\alpha_0 + R_{et}/R_\omega}{1 + R_{et}/R_\omega} \right)$.

The coefficient $\alpha_\infty = F_1 \alpha_{\infty,1} + (1 - F_1)\alpha_{\infty,2}$

where

$$\alpha_{\infty,1} = \frac{\beta_{i,1}}{\beta^*_\infty} - \frac{\kappa^2}{\sigma_{\omega,1}\sqrt{\beta^*_\infty}} \quad \text{and} \quad \alpha_{\infty,2} = \frac{\beta_{i,2}}{\beta^*_\infty} - \frac{\kappa^2}{\sigma_{\omega,2}\sqrt{\beta^*_\infty}}$$

The dissipation of $k\,(Y_k) = \beta^* k\omega$

where $\beta^* = \beta^*_i$ and $\beta^*_i = \beta^*_\infty \left(\frac{4/15 + \left(R_{et}/R_\beta\right)^4}{1 + \left(R_{et}/R_\beta\right)^4} \right)$

The dissipation of $\omega\,(Y_\omega) = \beta\omega^2$ where

$\beta = \beta_i$ and $\beta_i = F_1 \beta_{i,1} + (1 - F_1)\beta_{i,2}$.

The cross-diffusion term

$$D_\omega = 2(1 - F_1)\sigma_{\omega,2} \frac{1}{\omega} \frac{\partial k}{\partial x_j} \frac{\partial \omega}{\partial x_j}$$

The constants $\kappa = 0.41$, $\beta_{i,1} = 0.075$, $\beta_{i,2} = 0.0828$, $R_\beta = 8.00$, $\beta^*_\infty = 0.09$, $\sigma_{k,1} = 1.176$, $\sigma_{\omega 1} = 2.0$, $\sigma_{k,2} = 1.0$ and $\sigma_{\omega,2} = 1.168$

2.3 Reynolds Stress Model

The Reynolds stress model of Launder[5], *et al.* involves calculation of the individual Reynolds stresses, $\overline{u_i' u_j'}$, using differential transport equations. The modelled form is:

$$\frac{\partial u_k \overline{u_i' u_j'}}{\partial x_k} = D_{ij} + P_{ij} + \phi_{ij} - \varepsilon_{ij} \qquad (7)$$

where D_{ij}, P_{ij}, ϕ_{ij} represent, the diffusion, production, and pressure-strain process, respectively. Viscous dissipation is expressed as

$$\varepsilon_{ij} = \frac{2}{3}\delta_{ij}\varepsilon$$

where ε is the rate of dissipation of turbulent energy.

The production terms P_{ij} are given as

$$P_{ij} = -\left(\overline{u_i' u_j'} \frac{\partial u_j}{\partial u_k} + \overline{u_i' u_j'} \frac{\partial u_i}{\partial u_k} \right)$$

The pressure strain term is expressed as

$$\phi_{ij} = \phi_{ij1} + \phi_{ij2} + \phi_{ijw}$$

where

$$\phi_{ij1} = -C_1 \frac{\varepsilon}{k}\left(\overline{u_i' u_j'} - \frac{2}{3}\delta_{ij} k \right),\; \phi_{ij2} = -C_2 \left(P_{ij} - \frac{1}{3}\delta_{ij} P_{kk} \right)$$

and instead of ϕ_{ijw}, nonequilibrium wall function is used in FLUENT.

The diffusion of the Reynolds stress, D_{ij}, is approximated by

$$D_{ij} = \frac{\partial}{\partial x_k}\left(C_s \frac{k\overline{u_k' u_i'}}{\varepsilon} \frac{\partial \overline{u_k' u_j'}}{\partial x_i} \right)$$

The dissipation rate ε is governed by the following transport equation:

$$\frac{\partial u_k \varepsilon}{\partial x_k} = D_\varepsilon + \frac{\varepsilon}{k}\left(0.5 C_{\varepsilon 1} P_{kk} - C_{\varepsilon 2}\varepsilon\right)$$

where

$$D_\varepsilon = \frac{\partial}{\partial x_k}\left(C_\varepsilon \frac{k\overline{u_k' u_i'}}{\varepsilon} \frac{\partial \varepsilon}{\partial x_i} \right)$$

The model constants are

$$C_1 = 1.80, \quad C_2 = 0.60, \quad C_{s=} 0.18, \quad C_\varepsilon = 0.18,$$
$$C_{\varepsilon 1} = 1.44, \quad C_{\varepsilon 2} = 1.92$$

3. RESULTS & DISCUSSION

3.1 Flow through Axisymmetric Diffuser

As a first step towards computation of flow through an annular diffuser and volute exhaust, the turbulent swirling flow through a 12° included angle conical diffuser is numerically investigated and compared with the available experimental data of Senoo[6], *et al.* The experimental setup is shown in Fig. 2. They have measured:(a) the variations of axial and circumferential velocities in the constant area section ahead of diffuser (station A in Fig. 2), (b) the aforesaid two velocities at a station where the area ratio is four (station B in Fig. 2), and (c) pressure distribution along the wall and axis of the diffuser. Senoo[6], *et al.* defined the swirl parameter, m as

$$m = \frac{\int_0^R V_a V_z r^2 dr}{R\int_0^R V_a^2 r dr} \qquad (8)$$

where V_a and V_z are the axial and circumferential velocity components, respectively. It can be seen here that the product $m \times R$ represents the ratio of the angular momentum to the axial momentum passing through a pipe section of radius R. Here, r is the radial distance from the axis to any measurement point.

Armfield[7], *et al.* computed the flow through 12° included angle diffuser with low swirl number (m = 0.07).

The mean velocity and turbulence quantities were obtained using standard k-ε and algebraic stress model (ASM) with a two-layer wall function. The comparison between the predicted and the

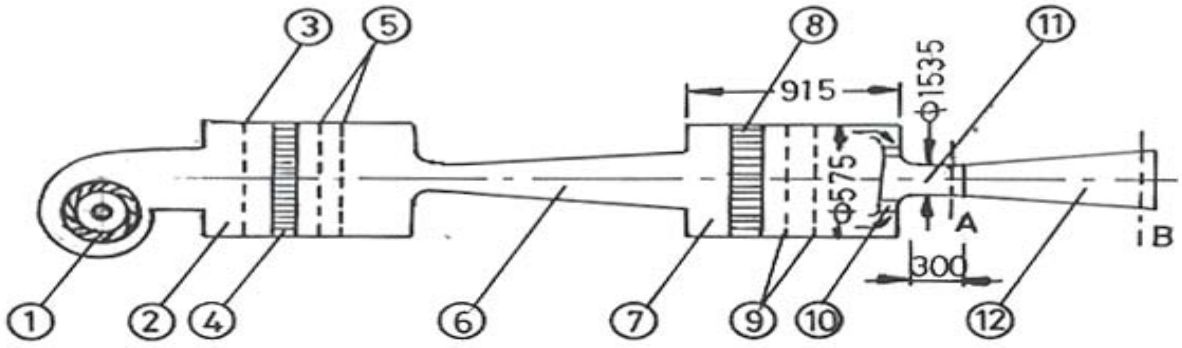

1. BLOWER
2&7. PLENUM CHAMBER
3,5&9. SCREEN
4&8. HONEYCOMB
6. VENTURI FLOW METER
10. SWIRL GENERATOR
11. TUBE.
12. DIFFUSER (CONE ANGLE 120).

Figure 2. Experimental setup

experimental data is reasonable with ASM model. However, to examine the model performance with higher swirl number, computations for m = 0.18 have been carried out in the present investigation.

Figure 3 shows the comparison of computed velocity profiles obtained by the models, viz, RNG k-ε model with modification for swirl, SST k-ω model, and RSM of turbulence with the experimental data at a station where the area ratio is four (station B in Fig. 2). It is seen that RSM and SST k-ω models show a close comparison with experimental data at different radial locations. However, the pressure loss is the important part of the present investigation and is discussed next.

Figure 4 shows the comparison of predicted and experimental static pressures along the diffuser wall. It is seen that the predictions by RNG k-ε and SST k-ω models are very close to the experimental distribution. It may be added that difference between pressures at stations A and B is a measure of the pressure loss along the diffuser. In this respect, prediction of SST k-ω model is almost exact. Further, Batten[8], *et al.* found the predictions of SST k-ω model and RSM model to be comparable in various practical cases. There is a trend towards increasing use of RSM, but Leschziner and Lien[9] pointed out that the use of RSM is more challenging in complex flows. Hence, SST k-ω model has been chosen for computation of flow in an annular diffuser and volute exhaust, as this model is economical in computational cost and time and also does not need wall treatment. In some cases, the results based on RNG k-ε are also presented.

3.2 Flow through Annular Diffuser & Volute Exhaust

For computation of flow through annular diffuser and volute exhaust (Fig. 1), the computational domain is discretised using unstructured grid containing 4,47,480 control volumes. The grid is shown in Fig. 5. The conditions at inlet and exit are: The inlet total temperature and total pressure are 300 K and 184.039 kPa (26.7 psia). At the outlet, the backpressure is equal to the local atmospheric pressure, ie, 90.985 kPa (13.2 psia). The inlet total temperature, total pressure, exit backpressure, and the experimental pressure distribution along some walls were provided by the funding agency. The effects of several parameters like inlet turbulent intensity, length of exit duct on the flow through annual diffuser were examined. These are described below.

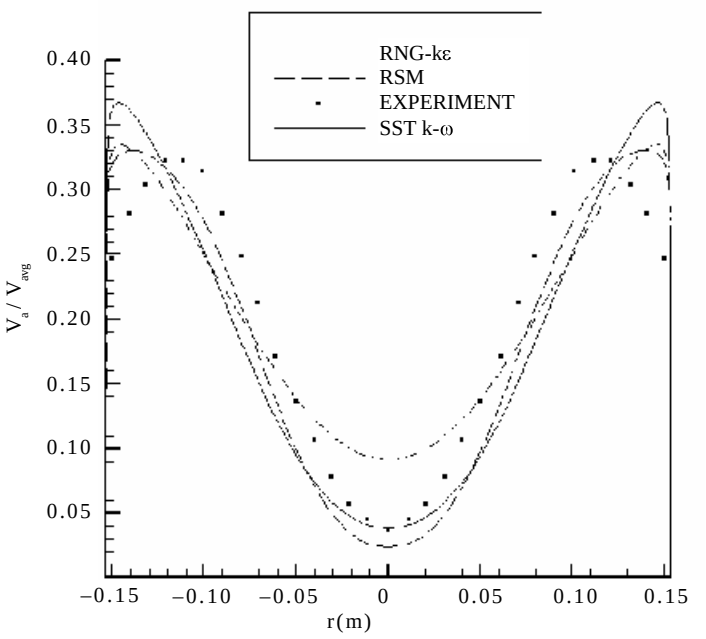

Figure 3. Axial velocity profiles with various models of turbulence (m = 0.18).

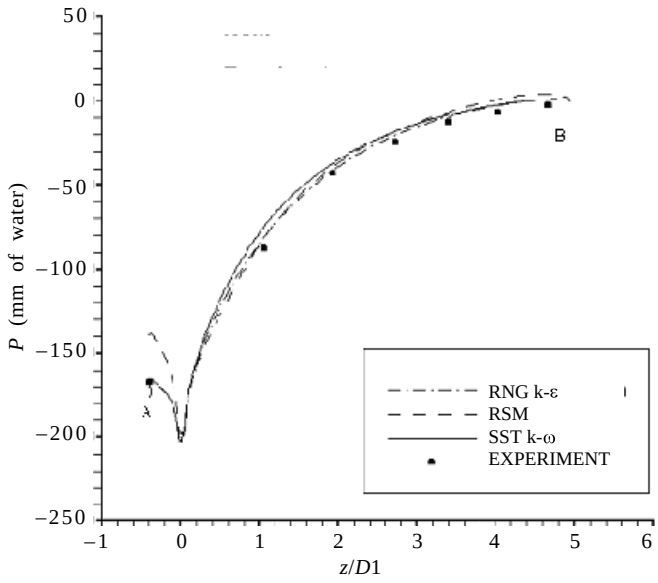

Figure 4. Static pressure along the diffuser wall

3.2.1 *Effect of Inlet Turbulent Intensity*

Computations with inlet turbulent intensity of 5 per cent and 10 per cent were carried out. No significant changes in the results were observed. Hence, inlet turbulent intensity of 10 per cent was used in the subsequent computations.

3.2.2 *Effect of Exit Duct Length*

To study the effect of exit pipe length on the predicted results, computations were carried out for the cases: (i) without exit pipe, (ii) exit pipe of one diameter length, and (iii) exit pipe of three diameter length. The exit backpressure was prescribed as atmospheric pressure. Computations showed that the static pressure over the exit suction was not uniform for cases (i) and (ii). The case (iii) gives desired uniform exit pressure over the entire cross section. It may be added that, unless an adequate exit pipe length is present, the pressure at the exit would not be uniform. The length of the exit pipe was not prescribed but it was mentioned that, during experiments, the exit pressure was uniform. Hence, the exit pipe of three diameter length was used in subsequent computations.

3.2.3 *Steady & Unsteady Computations*

Computations assuming steady state were performed using RNG k-ε and SST k-ω models for the given inlet total pressure of 26.7 psi. The wall static pressure along the inner diffuser and transition at 0 o'clock position has been shown in Fig. 6 (Fig. 1 for 0 o'clock position). It is evident from the figure that SST k-ω model predicts the wall static pressure closer to the experimental data than the RNG k-ε model. Computations were repeated assuming unsteady flow. Wall static pressures obtained along the inner diffuser and the transition for steady and unsteady cases at 0 O' clock positions is presented in Fig. 7. The comparison reveals that better results are obtained when the flow is treated as unsteady.

3.2.4 *Variation of Grid near the Wall*

The grid points were clustered adjacent to the wall to resolve the near-wall region. Computations were carried out for two grids having the point nearest to wall at (i) D_i / 800 and (ii) D_i / 3200 from the wall, where D_i is the hydraulic diameter of the inlet pipe. The pressures along the inner diffuser and transition at 0 O' clock position for the two grids are shown in Fig. 8. It is evident from the figure that there is no significant improvement in the results for the grid having the first point less than D_i /800 from the wall.

The wall static pressures along the inner diffuser and transitions at 3, 6, 9 O' clock positions are presented in Figs 9 to 11. Figures 12 and 13 show

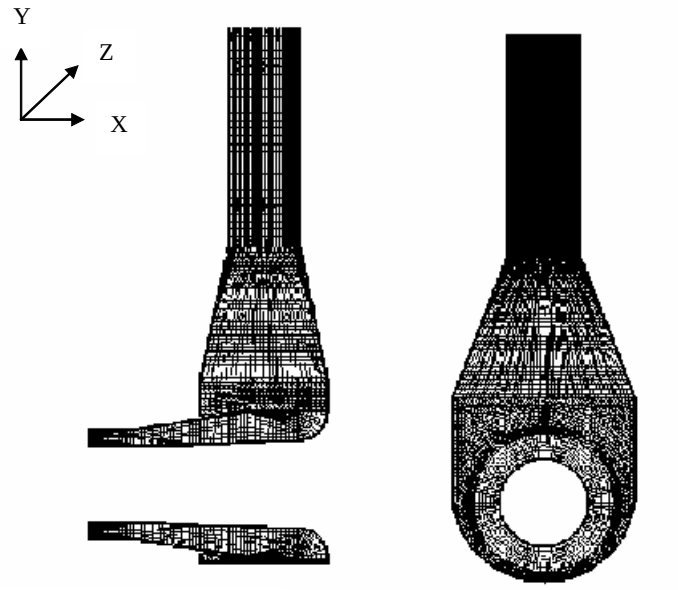

Figure 5. Grid

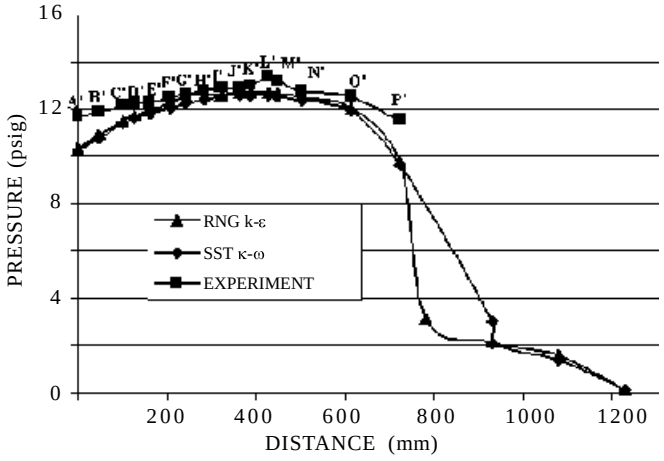

Figure 6. Pressures along the inner diffuser and transition at 0 O' clock position–steady flow computation.

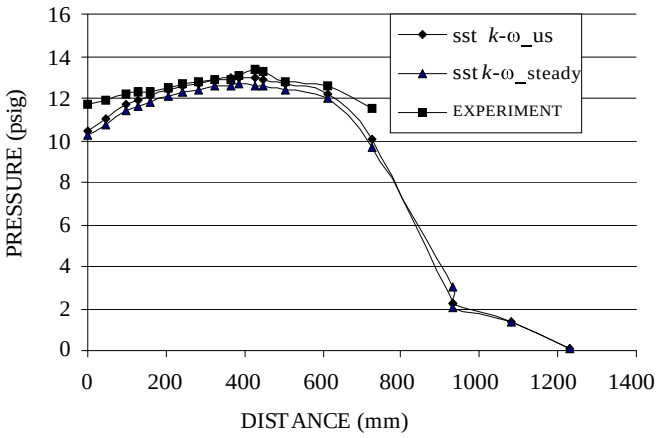

Figure 7. Pressures along the inner diffuser and transition at 0 O'clock position - unsteady flow computations.

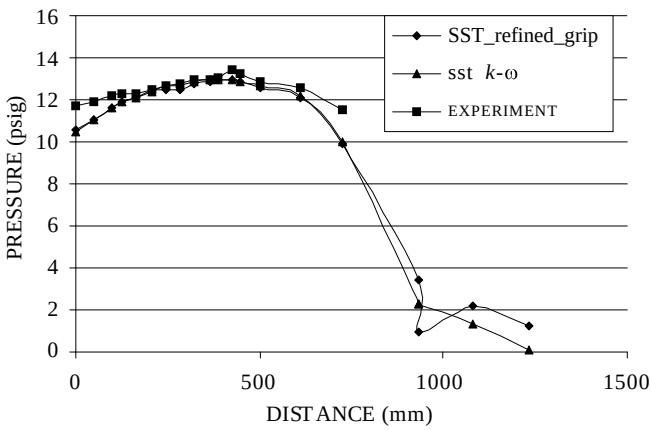

Figure 8. Pressures along the inner diffuser and transition at 0 O'clock position–influence of grid.

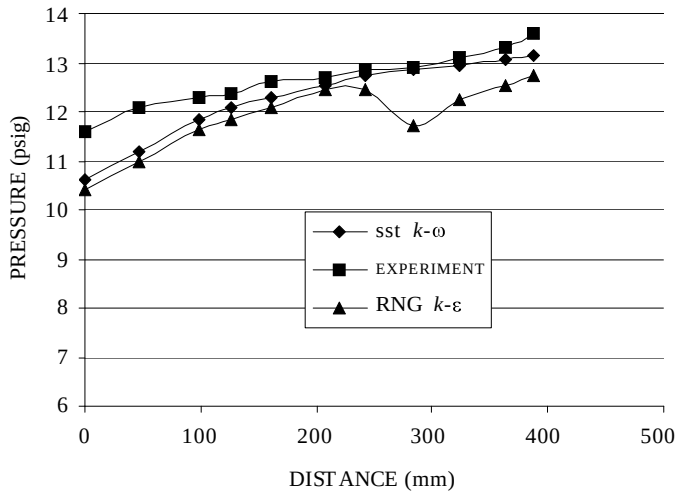

Figure 9. Pressures on the inner diffuser at 3 O'clock position

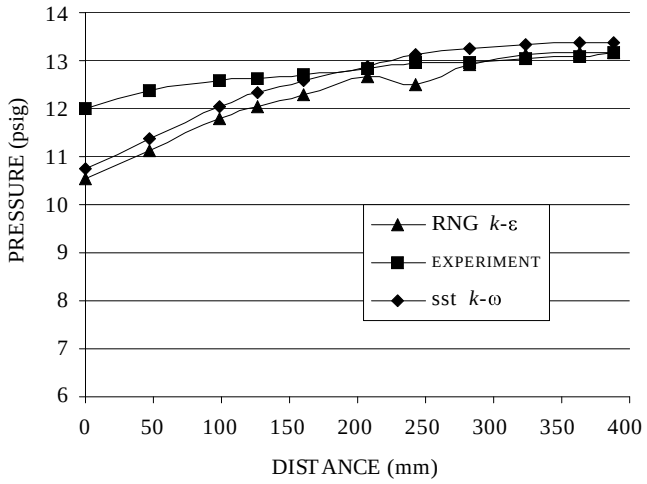

Figure 10. Pressures on the inner diffuser at 6 O'clock position

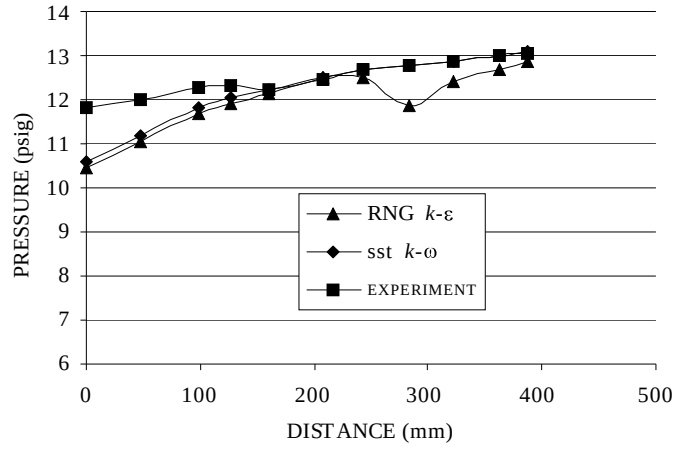

Figure 11. Pressures on the inner diffuser at 9 O'clock position

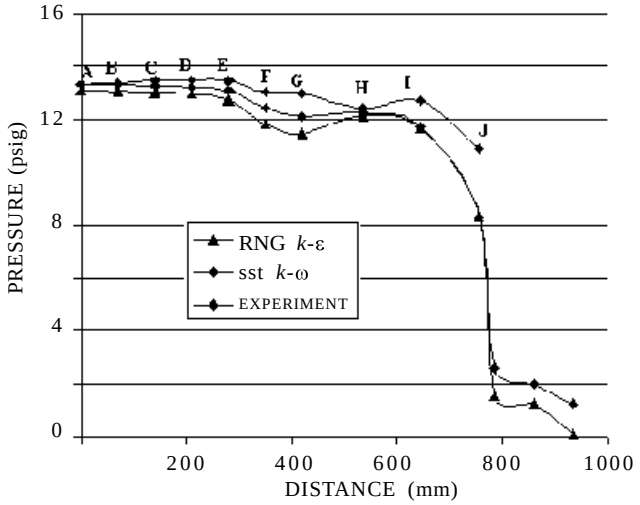

Figure 12. Pressure distribution along right half of the volute casing and transition duct wall.

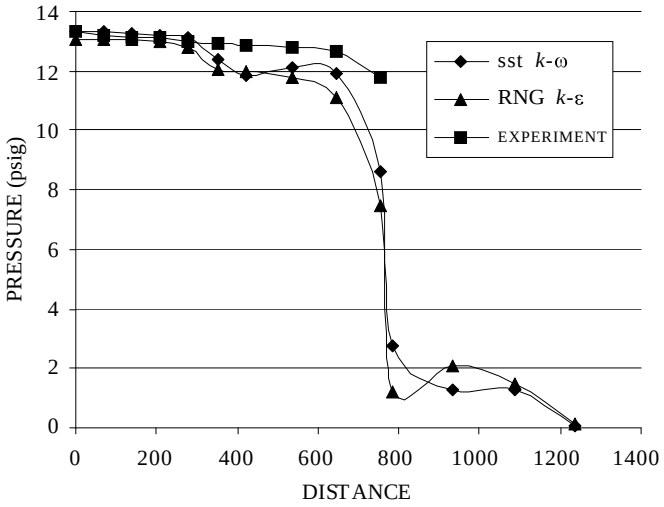

Figure 13. Pressure distribution along left half of the volute casing and transition duct wall.

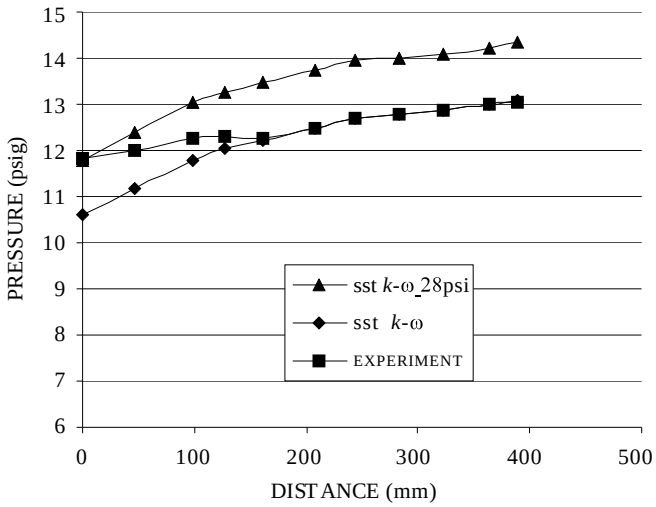

Figure 14. Pressures on the inner diffuser at 9 O'clock position-influence of inlet pressure.

the wall static pressure distributions along right and left half of the volute casing and transition duct.

3.2.5 *Variation of Inlet Total Pressure*

The mass flow rate through the duct is an important parameter. The information about it is not available from the experimental data. The computations give a mass flow rate of 6.813 kg/s for the total pressure of 26.7 psi at the inlet (Fig. 1). However, computed results indicate that the computed static pressure near the inlet [point A in Fig. 1(b)] is lower by about 1 psi as compared to the experimental value (Fig. 7). To examine the possible effect of this difference on the mass flow rate, the prescribed total pressure at the inlet was increased from the experimental value of 26.7 psi. For an inlet total pressure of 28 psi, the computed static pressure at point A matched with the experimental value (Fig. 14), although the subsequent variation was higher than the experimental distribution. With this inlet total pressure, the mass flow rate was

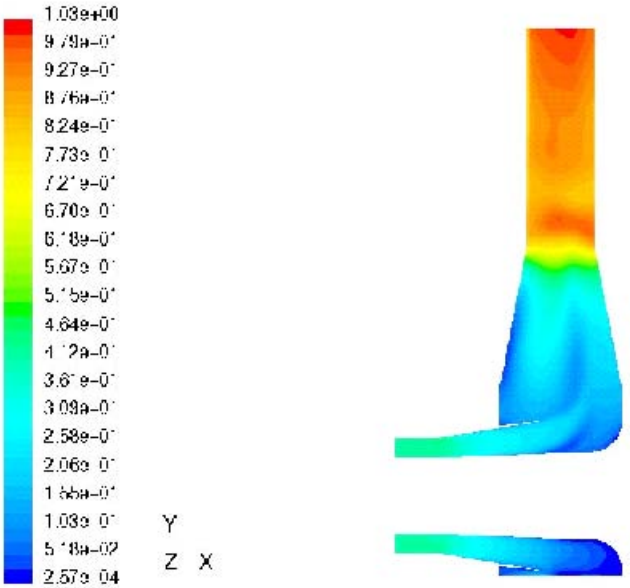

Figure 15. Mach contours at the central plane

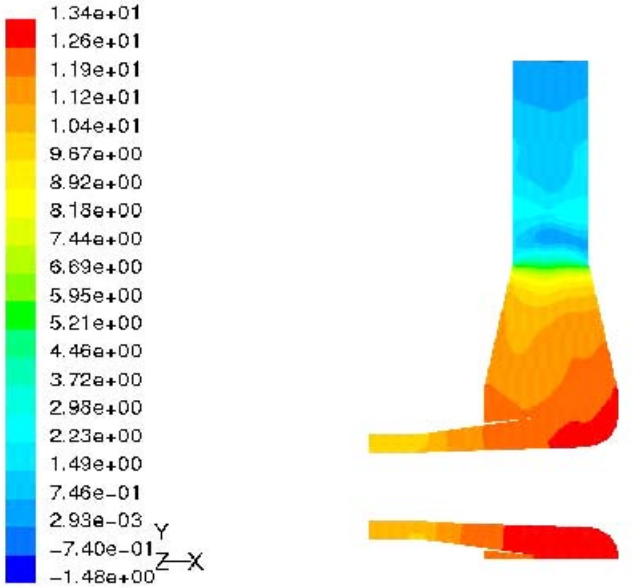

Figure 16. Static pressure contours at the central plane (psi)

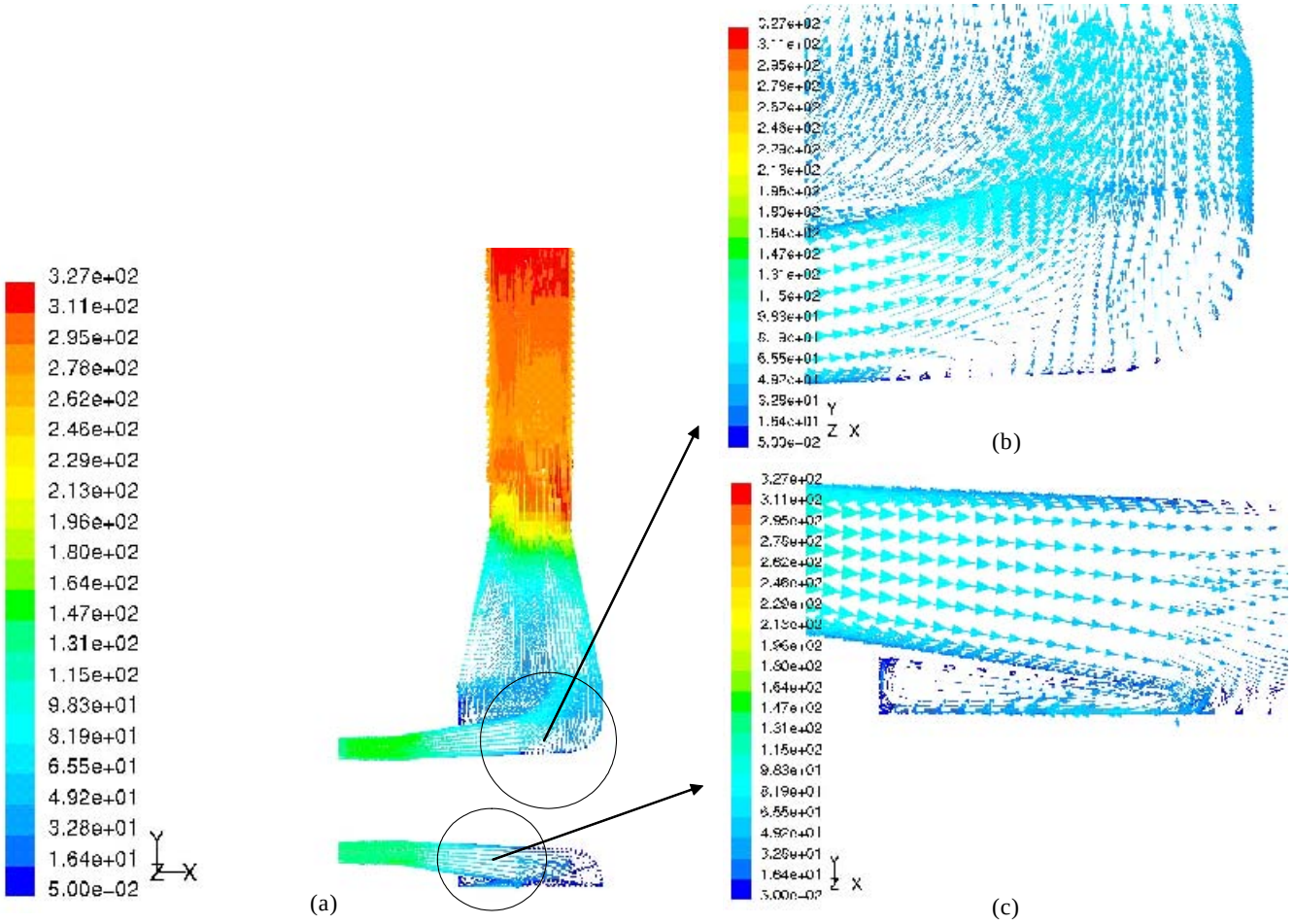

Figure 17. Vector plot at the centre plane and flow separation: (a) overall pattern, (b) detail near exit of annular diffuser, and (c) detail near extended circular lip.

7.238 kg/s, which is only 6 per cent higher than in the earlier case with inlet pressure of 26.7 psi. Thus, it is interesting to note that SST k-ω model gives reasonable predictions of wall static pressure and the mass flow rate can be expected to be within 6 per cent of the correct value.

3.3 Flow Features

The Mach contours in the central plane of the volute exhaust are shown in Fig. 15. The flow is subsonic throughout but reaches sonic value near the exit. Figure 16 shows the static pressure contours in the central plane of the volute exhaust. Figure 17 (a) presents the velocity vector in the central plane ($Z = 0$). The flow from the annular diffuser separates from the inner wall near the exit of the annular diffuser [ie, near point *F'* in Fig. 1(b)]. The onset of flow separation is seen in Fig. 17 (b). This recirculation region of relatively low velocity results in static pressure loss. Figure 17 (c) reveals a recirculation region at the central plane and in between the extended circular lip and the bottom circular casing. Thus, the flow field is unsteady, complementing the observation that unsteady computation gives better results.

4. CONCLUSIONS

The computations considering flow as unsteady and using SST k-ω model of turbulence give the results of wall static pressure distributions along the inner wall of annular diffuser, the volute casing, and the transition duct wall, which are in close agreement with the experimental results. The predicted mass flow rate is expected to be within 6 per cent of the actual flow rate. It is planned to use this technique for optimising geometry of volute exhaust in practical engines.

ACKNOWLEDGEMENTS

This project was funded by the Gas Turbine Research Establishment (GTRE), Bangalore. Dr S. Kishore Kumar/ Vimala Narayanan were the project monitors. The computations were carried out at the CFD Centre, IIT Madras, Chennai. The support is gratefully acknowledged.

REFERENCES

1. Arun, M.; Tulapurkara, E.G., Sundararajan, T., & Senthil Kumar, K. Computation of turbulent swirling flow in a conical diffuser. *In* Proceedings of the 2nd International and 29th National Conference on Fluid Mechanics and Fluid Power, IIT Roorkee, December 12-14, 2002. pp. 401-08.

2. Arun, M. & Tulapurkara, E.G. Computation of turbulent flow inside an enclosure with central partition. *Progress in CFD*, 2005, **32**, 455-65.

3. Yakhot, V. & Orszag, S.A. Renormalisation group analysis of turbulence. I. Basic theory. *J. Sci. Comput.*, 1986, **1**, 3-51. (see also Choudhury, D. Introduction to renormalisation group method and turbulence modelling. Fluent Inc, Technical Memorandum, TM-107, 1993.)

4. Menter, F.R. Two-equation Eddy-viscosity models for engineering applications. AIAA *Journal*, 1994, **32**, 1598-605.

5. Launder, B.E.; Reece, G.J. & Rodi, W. Progress in the development of Reynolds stress turbulence closure. *J. Fluid Mechanics*, 1975, **68**, 537-86.

6. Senoo, Y.; Kawaguchi, N. & Nagata, T. Swirl flow in conical diffusers. *Bull. Japan Soc. Mech. Engg.*, 1970, **21**, 112-19.

7. Armfield, S.W.; Cho, N.H. & Fletcher, C.A.J. Prediction of turbulence quantities for swirling flow in conical diffusers. *AIAA Journal*,1990, **28**, 453-60.

8. Batten, P.; Craft, T.J.; Leschziner, M.A. & Loyau, H. Reynolds stress transport modeling for compressible aerodynamic applications. *AIAA Journal*, 1999, **37**, 785-97.

9. Leschziner, M.A. & Lien F.S. Numerical aspects of applying second moment closure to complex flows in closure strategies for turbulent and transitional flows, edited by B.E. Lander and N.P. Sandham. Cambridge University Press, 2002. pp. 153-87.

Contributers

Mr M. Arun did his BE(Mech) from the Regional Engineering College, Surat, and MS (Aero Engg) from Indian Institute of Technology Madras, Chennai. Presently, he is doing PhD at the University of Greenwich, UK, in the area of combustion. He has published 4 papers in national/international journals/conference proceedings. His research interests are: Computational fluid dynamics, combustion, and parallel computing.

Prof E.G. Tulapurkara received his BE (Mech) from the Vikram University Ujjain, ME (Aero Engg) from the IISc, Bangalore, and PhD (Aero Engg) from the IIT Madras, India. He was chairman, Dept of Aerospace Engg at IIT Madras from 1995-98 and Principal Coordinator, CFD Centre, IIT Madras from 1998-2005. He has more than 120 papers in refereed journals and conference proceedings. He is a fellow of the Aeronautical Society of India and associate fellow of the American Institute of Aeronautics and Astronautics and was President of the National Society of Fluid Mechanics and Fluid Power (2004-2005). His research interests include measurement and computation of turbulent flows.

Prof T. Sundararajan obtained his PhD (Mech Engg) from the University of Philadelphia, USA, in 1983. He worked as a postdoctoral fellow at the University of Philadelphia, USA, from 1983–84. He joined as Assistant Professor at the Indian Institute of Technology, Kanpur, in 1985. Presently, he is working at the Institute of Technology, Madras, as Professor. He has guided 17 students for their PhD and 24 students for their MS. He has published 76 research papers in various journals and presented 85 papers in various conferences. He has also published a textbook on computational fluid dynamics. His areas of research include: Spray combustion, jet flows, heat transfer and fluid flow in porous media, and thermal modelling of manufacturing and metallurgical problems. He is an elected fellow member of the Indian National Academy of Engineering since 2003.